

Opportunistic retrospective assessment of HUAC, bone density, SFT and breast density on CT images and relationship with severity of COVID-19

Mahmut Subasi¹, Mustafa Duger², Cengiz Erol³, Irmak Durur-Subasi^{3*}

¹ Department of Thoracic Surgery, Istanbul Medipol University, Istanbul, Turkey

² Department of Pulmonology, Istanbul Medipol University, Istanbul, Turkey

³ Department of Radiology, Istanbul Medipol University Faculty of Medicine, Istanbul, Turkey

ABSTRACT



Aim. To evaluate mean Hounsfield unit calculation (HUAC), bone density, subcutaneous fat thickness (SFT), breast density (constitutional imaging biomarkers) and age in symptomatic patients with COVID-19, to assess their correlation with pneumonia severity. **Materials and Methods.** Between 11 March and 30 May 2020, 272 consecutive symptomatic female patients with COVID-19 who underwent chest CT imaging at baseline were reviewed. HUAC, bone density, SFT and breast density were evaluated retrospectively and statistically compared in cases with negative/positive PCR test results, with/without pneumonia and with mild/moderate-severe pneumonia. Univariate/multivariate logistic regression analyses were applied for estimation of moderate/severe pneumonia. **Results.** The parameters of age, HUAC, bone density, SFT and breast density were significantly different between patients with/without pneumonia. Additionally, the patients with moderate-severe pneumonia were older, had lower bone density, lower HUAC values, greater SFT and mostly fatty breast density. ROC analysis showed the highest AUC values of 0.763 and 0.744 for age and HUAC, respectively. A combination of HUAC and age was the most accurate model for estimation of moderate/severe pneumonia on logistic regression. Good intraobserver and interobserver reliabilities were detected. **Conclusions.** The severity of COVID-19 pneumonia among adult females was associated with older age, lower bone density, a lower HUAC value, greater SFT and fatty breast parenchyma. All these factors can be responsible for 21.9% of the development of moderate/severe pneumonia.

Category: Original Research Paper

Received: November 28, 2022

Accepted: January 26, 2023

Published: April 25, 2023

Keywords:

breast density, COVID-19, sarcopenia, osteoporosis

*Corresponding author:

Irmak Durur-Subasi,

Department of Radiology, International Faculty of Medicine,
Istanbul Medipol University, TEM Avrupa Otoyolu, Goztepe
Cikisi No:1, Bagcilar, Istanbul, Turkey

E-mail: isubasi@medipol.edu.tr

Introduction

From late 2019, coronavirus disease-2019 (COVID-19) quickly changed daily life and medical routines worldwide. The proportion of women among COVID-19 patients was lower in the geographies where the disease spread [1]. This fact caught our attention in our daily radiology routine during the COVID-19 pandemic. If a chest computed tomography (CT) scan was performed on a young woman, the expectation was that there would be no pneumonia or at most a mild pneumonia form. It has been reported that women are vulnerable but have less severe disease and a lower fatality rate [2]. It is clear that the gender distribution of COVID-19 appeared to be unbalanced. Men are reported to have higher mortality rates (60-70% deaths) [3,4]. The underlying causes might include gender dimorphism in immunity, immunomodulatory effects of sex hormones, smoking, diabetes and social role [3].

While the pandemic continued, the question of where this difference originates began to be investigated. In addition to different sex-specific mortality rates, the confirmed cases of SARS-CoV-2 infection differed between males and females across age groups. A higher incidence is observed in the female group at the age of 10-50 years, in males under 10 and in males after 50 years [5]. On the other hand, men display delayed viral clearance [6,7]. Women seem to mount a stronger immune response (immunoglobulins protect them from the occurrence of virus-induced damage) but exhibit lower proinflammatory cytokine release (thus protecting them from immune-mediated damage occurring at a later time). In particular, men show increased type 1 cytokine production (IFN- γ , IL-2). Another mechanism may be the immunomodulatory effects of sex hormones. It was confirmed in an experimental mouse model that elevated 17 β -oestradiol protects females from influenza by suppressing

inflammatory responses. A correlation between low 17β -oestradiol levels and increased CD16 expression (and consequently, proinflammatory cytokines) has been found [3]. Oestrogen is the primary female sex hormone. Its responsibilities are progressing and governing the female reproductive system and secondary sex characteristics. Additionally, its relationships with age, muscle density, bone density, subcutaneous fat thickness and breast density have been defined. All these features can be evaluated using radiological imaging methods. To the best of our knowledge, no other study in the English literature has described these structural features and correlated the radiological severity of COVID-19 pneumonia.

Materials and Methods

This retrospective single-center study was approved by the Ministry of Health (2020-06-22T16_19_42) and the institutional review board (6.8.2020/566), and written informed consent was waived due to both the retrospective design and the emergence of epidemic outbreaks.

Patients

Our University Hospital is located in Bagcilar, the principal zone of the COVID-19 outbreak in Istanbul. Between 11 March 2020 and 30 May 2020, 272 consecutive female patients with an initial diagnosis of COVID-19 (based on clinical features and CT or a positive PCR test) were evaluated. Although symptomatic, patients with both negative PCR results and no CT findings ($n=106$), patients who were evaluated by CT with the aim of preoperative evaluation ($n=3$) and one patient who was confirmed to have a different pneumonia ($n=1$), for a total of 110 patients, were excluded from the study. A total of 162 patients were enrolled (Figure 1). The ages, symptoms, acute phase reactant levels (if any, such as CRP, D-dimer levels, ESR, ferritin, and procalcitonin), and PCR results evaluated during the patients' admission were recorded.

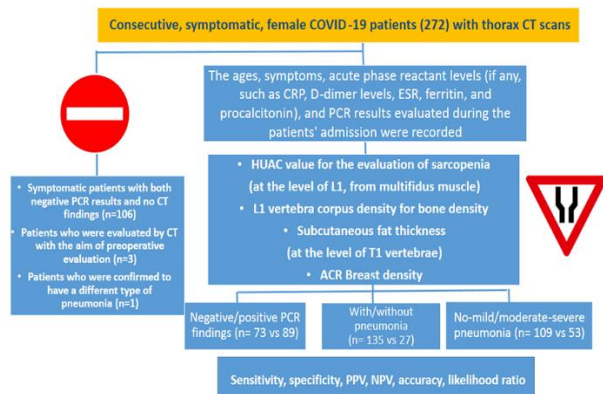


Figure 1. Flowchart of the study. Hounsfield unit average calculation (HUAC), bone density, and subcutaneous fat thickness were evaluated.

Computed Tomography

All thorax CT scans were acquired in the supine position with a Philips Brilliance BigBore 16-slice

machine during admission of the patient. A 16×0.625 -mm collimation, 360 mm field of view (FOV), and 1.0-mm section thickness were used. The scan time was approximately 10 s. Through a single breath hold, the lungs, from the level of the apices of the lungs to below to the diaphragmatic level, were scanned. For interpretation, standard lung and mediastinal windows were assessed.

The chest CT indications were determined according to the Ministry of Health's recommendations. A radiologist (IDS) who did not know the RT-PCR results interpreted the CT images. Thorax CT images were classified as positive or negative in terms of COVID-19 pneumonia. The typical features of pneumonia, including ground-glass opacities, multifocal patchy consolidation, and/or interstitial changes with a peripheral distribution, and the classical clinical scenario (clinical symptoms, such as fever, cough, fatigue and/or shortness of breath, or positive close contact with a COVID-19 patient), were accepted as findings of COVID-19 pneumonia [8].

Image Analysis

CT images were retrospectively analyzed using a commercially available picture archiving and communication system (Centricity, RIS, GE Healthcare). With a semiquantitative scoring system, the extension of pulmonary involvement was appraised. Every pulmonary lobe was evaluated and scored as follows: 0, no; 1, less than 5%; 2, 5–25%; 3, 26–50%; 4, 51–75%; and 5, 76–100% involvement. The scores for the lobes were summed, and a CT severity score ranging from 0 (no involvement) to 25 (maximum involvement) was obtained. CT severity scores of 1–5, 6–14, and 15–25 indicated mild, moderate and severe involvement, respectively [9].

The Hounsfield unit average calculation (HUAC) was calculated from the multifidus muscle at the level of L1 for evaluation of sarcopenia using the initial CT scans of the patients and the following formula:

$$\text{HUAC} = (\text{right area} \times \text{density}) + (\text{left area} \times \text{density}) / \text{total area}$$

For the bone density measurements, CT attenuation of the L1 vertebra was measured in Hounsfield units (HU) by insertion of an oval region of interest (ROI) within a transverse section of the vertebral medulla by first locating the midvertebral body in the sagittal plane. ROIs were made as large as possible while avoiding vertebrobasilar structures and cortical surfaces [10] (Figure 2).

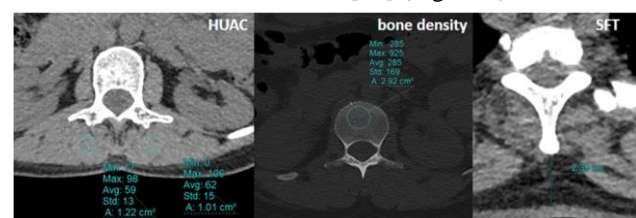


Figure 2. Hounsfield unit average calculation (HUAC), bone density and subcutaneous fat thickness (SFT) measurements.

The subcutaneous fat thickness (SFT) was measured from the level of the T1 vertebra as the maximum length from the spinous process of the vertebra to the skin.

Breast densities were evaluated on sagittal reformat CT images based on the American College of Radiology (ACR) breast magnetic resonance imaging definition (Figure 3). ACR densities of A and B were accepted as fatty, and ACR densities of C and D were considered dense patterns.

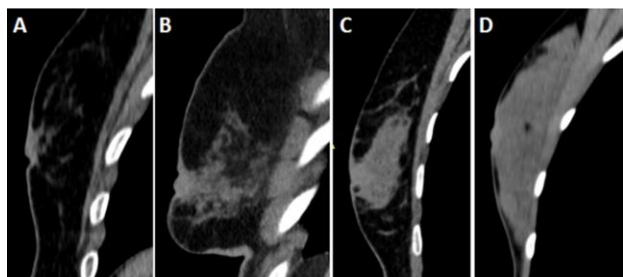


Figure 3. Breast densities on CT images were evaluated using sagittal reformat images.

Statistical Analysis

Statistical analysis was performed using SPSS 16.0 software. Continuous variables were displayed as the mean±standard deviation, and categorical variables are reported as counts and percentages. To confirm the distribution of the data, the one-sample Kolmogorov–Smirnov test was performed. When a normal distribution was not confirmed, log transformation was used.

The parameters of age, HUAC, bone density, and SFT were compared in cases with negative/positive PCR results, with/without pneumonia and with mild/moderate-severe pneumonia using an independent samples t-test. Breast density was compared using a chi-square test. A receiver operating characteristic (ROC) analysis was performed to evaluate the diagnostic capabilities for estimating moderate-severe pneumonia. Cut-off values, sensitivity, specificity, positive and negative predictive values, accuracy and the likelihood ratio for estimation of moderate-severe pneumonia were analyzed.

All variables that were identified as significant ($p < 0.05$) via an independent samples t-test or chi-square test were considered candidates for univariate or multivariate analysis using a binary logistic regression model. We conducted binary logistic regression to validate constitutional parameters (age and imaging biomarkers) for estimation of moderate/severe pneumonia. The correlation coefficients were under 0.700 and VIF<3; therefore, multicollinearity was ruled out. Four different models were considered, and the beta, standard error, t, R², P value, accuracy, sensitivity, and specificity values of the models were calculated. All analyses were two-sided, and $p < 0.05$ was considered statistically significant.

Intra- and interobserver correlations were revealed by Pearson correlation for each parameter except breast density. The latter was evaluated using Cronbach's α .

Results

A total of 162 female patients (between the ages of 18–90, mean±standard deviation 47±16) were enrolled.

All the patients had classical clinical symptoms of COVID-19 (Table 1). The most common symptoms for this group of patients were cough ($n = 80$, 49.4%), weakness ($n = 67$, 41.4%), fever ($n = 58$, 35.8%) and dyspnoea ($n = 37$, 22.8%). The most encountered comorbidities were hypertension ($n = 22$, 13.6%), chronic lung disease ($n = 19$, 11.7%), diabetes mellitus ($n = 14$, 8.6%), and coronary artery disease ($n = 11$, 6.8%). No pregnant patients were included in the study. One patient was lactating and had mild pneumonia, and she was treated as an outpatient. Patients with moderate/severe pneumonia ($n = 53$) were offered hospitalization, followed up and treated, and three of these patients died.

Table 1. Features of the included patient population.

Age	18–90 years old (47±16)	
Symptoms	Cough ($n = 80$, 49.4%) Weakness ($n = 67$, 41.4%) Fever ($n = 58$, 35.8%) Dyspnoea ($n = 37$, 22.8%) Muscle-bone-joint pain, back pain ($n = 31$, 19.1%) Sore throat ($n = 28$, 17.3%) Loss of sense of taste/smell ($n = 27$, 0.6%) Headache ($n = 22$, 13.6%) Emesis ($n = 13$, 8%) Chest pain ($n = 10$, 6.2%) Others (palpitation, conjunctivitis, hoarseness, loss of appetite, enteritis) ($n = 10$, 6.2%)	
Comorbidities	Hypertension ($n = 22$, 13.6%) Chronic lung disease ($n = 19$, 11.7%) Diabetes mellitus ($n = 14$, 8.6%) Coronary artery disease ($n = 11$, 6.8%) Arrhythmia ($n = 5$, 3%) Chronic kidney disease ($n = 3$, 1.8%) Others (Alzheimer's disease, acute myeloblastic leukaemia, Hashimoto thyroiditis, hereditary polyneuropathy, hyperlipidaemia, chronic hepatitis, migraine, mitral stenosis, rheumatoid arthritis, vertigo) ($n = 12$, 7.2%)	
PCR test results	73 negative (45%), 89 positive (55%)	
Hospitalization	24 patients	
Exitus	3 patients	
Oestrogen-related imaging biomarkers	HUAC	-73–64 (mean±SD of 43±16) HU
	Bone density	29–327 (mean±SD of 186±65) HU
	SFT	3–59 (mean±SD of 20±9) mm
	Breast pattern	ACR type A ($n = 36$, 22.2%) Fatty breast type ACR type B ($n = 45$, 27.8%) ($n = 81$, 50%) ACR type C ($n = 62$, 38.3%) Dense breast type ACR type D ($n = 37$, 22.8%) ($n = 81$, 50%)
ACR: American College of Radiology, HUAC: Hounsfield unit average calculation, PCR: polymerase chain reaction SFT: subcutaneous fat thickness.		

SARS-COV2 PCR tests were negative for 73 patients (45%) and positive for 89 patients (55%). The parameters

of age ($p = 0.625$), HUAC ($p = 0.929$), bone density ($p = 0.687$), SFT ($p = 0.925$) and ACR breast density ($p = 0.875$) were not different between PCR-negative and PCR-positive patients (Table 2).

Table 2. Comparison of age, HUAC, bone density, adipose tissue thickness and breast density between patients with different PCR and CT findings (* statistically significant results).

	SARS-COV2 PCR n= 162			CT involvement (pneumonia-/+) n= 162			CT involvement score (mild/moderate-severe pneumonia) n= 135		
	Negative (n=73, 45%)	Positive (n=89, 55%)	P value	Pneumonia- (n=27, 17%)	Pneumonia+ (n=135, 83%)	P value	Mild pneumonia (n=82, 61%)	Moderate/severe pneumonia (n=53, 39%)	P value
Age (year-old)	47±15	46±16	0.625	36±14	49±15	<0.001*	43±14	57±13	<0.001*
HUAC (HU density)	43±13	43±19	0.929	51±9	41±17	<0.001*	47±9	32±22	<0.001*
Bone density (HU density)	184±67	188±62	0.687	221±51	179±65	0.001*	190±61	161±67	0.01*
SFT (mm)	20±9	20±10	0.925	16±9	20±9	0.029*	19±8	23±11	0.009*
Breast Density	%49 ACR A-B %51 ACR C-D	%51 ACR A-B %49 ACR C-D	0.875	%33 ACR A-B %67 ACR C-D	%53 ACR A-B %47 ACR C-D	0.06	%44 ACR A-B %56 ACR C-D	%68 ACR A-B %32 ACR C-D	0.008*

CT: computed tomography, HUAC: Hounsfield unit average calculation, PCR: polymerase chain reaction, SFT: subcutaneous fat thickness.

Overall, 27 of the patients (17%) had no findings of pneumonia. All were positive for SARS-COV2 based on PCR testing. A total of 135 patients (83%) had classical or possible CT findings of SARS-COV2 pneumonia. Patients with CT findings of SARS-COV2 pneumonia had a PCR negativity rate of 54% ($n=73$) and positivity rate of 46% ($n=62$). This difference was representative of the study population because, although symptomatic, patients with negative PCR results and no CT findings ($n=110$) were excluded from the study.

All parameters were significantly different between the patients with negative ($n=27$, 17%) and positive ($n=135$, 83%) CT findings. Patients with pneumonia were older (mean±SD of 49±15, $p < 0.001$), had a lower HUAC value (mean±SD of 41±17, $p < 0.001$), had lower bone density (mean±SD of 179±65, $p = 0.001$), and had a greater SFT (mean±SD of 20±9, $p = 0.029$). All differences were significant (Table 2). Patients with pneumonia had fatty breast density more commonly (53% vs 33%), but the difference was not significant ($p=0.06$).

Among the female patients with COVID-19 pneumonia ($n=135$), CT findings showed mild disease for 82 patients (61%), moderate disease for 37 patients (27%) and severe

disease for 16 patients (12%). Patients with moderate-severe pneumonia ($n=53$) were older (mean ± SD of 57 ± 13, $p < 0.001$), showed a lower HUAC value (mean±SD of 32±22, $p < 0.001$), lower bone density (mean±SD of 161±67, $p = 0.01$), and greater SFT (mean±SD of 23±11, $p = 0.009$). Patients with moderate-severe pneumonia had fatty breast density more commonly than patients with mild pneumonia (68% vs 32%, $p=0.008$) (Table 2). All the differences were significant.

Based on ROC analysis, for estimation of moderate-severe pneumonia, the area under the curve values from highest to lowest were as follows: age (0.763), HUAC (0.744), bone density (0.630) and SFT (0.616) (Table 3, Figure 4). The threshold values were 47 years old for age, 45 HU for HUAC, 183 HU for bone density and 18.5 mm for SFT. The most accurate parameter to estimate moderate-severe pneumonia was HUAC, with an accuracy rate of 68%. The most sensitive parameter was age, with a sensitivity of 75%, and the most specific was HUAC, with a specificity of 66%. The highest PPV went to HUAC (57%), and the NPV went to age (80%). The positive likelihood ratio for age and HUAC was ≥ 2.00 .

Table 3. ROC results for estimation of moderate-severe pneumonia.

	AUC	95% CI	Threshold	Sens (%)	Spec (%)	PPV (%)	NPV (%)	Acc (%)	Pos LR	95% CI
Age	0.763	0.684-0.842	≥ 47 -y-o	75	62	56	80	67	2.00	1.45-2.74
HUAC	0.744	0.656-0.834	≤ 45 HU	71	66	57	78	68	2.08	1.47-2.95
Bone density	0.630	0.532-0.729	≤ 183 HU	68	49	46	70	56	1.33	1.00-1.76
SFT	0.616	0.517-0.714	≥ 18.5 -mm	64	50	45	68	56	1.28	0.95-1.72

Acc: accuracy, AUC: area under the curve, CI: confidence interval, PPV: positive predictive value, Pos LR: positive likelihood ratio, Sens: sensitivity, Spec: specificity. The highest values are given in bold.

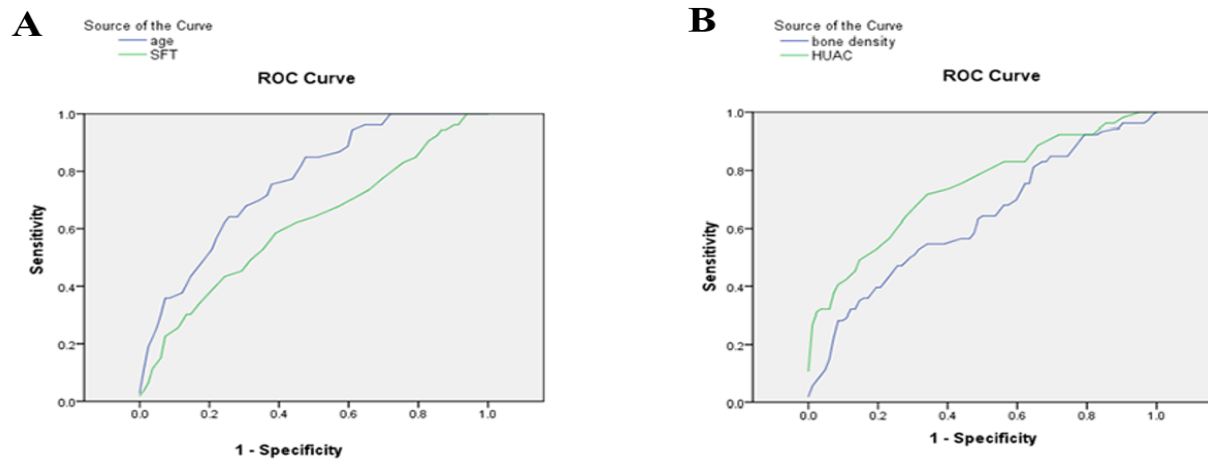


Figure 4 (A, B). ROC curves for age, SFT, HUAC and bone density.

We conducted univariate/multivariate logistic regression analyses to validate the age- and constitutional imaging biomarkers for estimation of moderate/severe pneumonia. The model showed an accuracy of 69.4% in estimating moderate-severe pneumonia, and the

contribution of the model for estimation of moderate/severe pneumonia was 21.9%. Another model utilizing age and HUAC demonstrated a similar performance. Individually, the parameters (age and HUAC) showed a lower but similar performance (Table 4).

Table 4. Results of different regression models for predicting moderate/severe pneumonia.

Model	Parameter	Beta	SE	Exp (B)	R2	P	A (%)	Sens (%)	Spec (%)
1	Age (≥ 47 yo)	1.622	0.392	5.062	0.178	<0.001*	67.4	75.5	62.2
2	HUAC (≤ 45 HU)	1.560	0.385	4.757	0.169	<0.001*	67.9	71.2	65.9
3	Age (≥ 47 yo) HUAC (≤ 45 HU)	1.027 0.965	0.478 0.470	2.792 2.624	0.210	0.032 0.040	69.4	73.2	63.5
4	Age (≥ 47 yo) Breast density (fatty) Bone density (≤ 183 HU) HUAC (≤ 45 HU) SFT ≥ 18.5 -mm	1.137 -0.325 -0.389 0.920 0.020	0.550 0.499 0.489 0.432 0.451	3.118 0.678 2.509 1.020 0.723	0.219	0.039 0.471 0.436 0.060 0.963	69.4	73.2	63.5

There were good intra- and interobserver reliabilities for HUAC ($R=0.782$, $p<0,001$ and $R=0.807$, $p<0,001$, respectively), bone density ($R=0.857$, $p<0,001$ and $R=0.878$,

$p<0,001$, respectively), fat tissue thickness ($R=0.973$, $p<0,001$ and $R=0.953$, $p<0,001$, respectively) and breast density (Cronbach's α 0.93 and 0.97, respectively) (Table 5).

Table 5. Intra/interobserver reliability analyses.

	Pearson Correlation Coefficient			Cronbach's α
	HUAC	Bone density	SFT	Breast density
Intraobserver reliability	$R=0.782$ $p<0,001$	$R=0.857$ $p<0,001$	$R=0.973$ $p<0,001$	0.93
Interobserver reliability	$R=0.807$ $p<0,001$	$R=0.878$ $p<0,001$	$R=0.953$ $p<0,001$	0.97

Discussions

In our study, we found that adult females with moderate-severe COVID-19 pneumonia were older and had lower bone density (osteopenic), lower HUAC values (sarcopenic), greater SFT (obese) and fatty breast parenchyma during their initial evaluation. To predict moderate/severe pneumonia, while the parameter of age provided the most sensitive results, HUAC had the most specific results, and the "HUAC and age" combination was the most accurate.

COVID-19 is associated with a mortality rate of 1-3% and frequently associated with acute respiratory distress syndrome. This is attributed to an uncontrolled immune response, the so-called "cytokine storm". Senility, diabetes, hypertension, and obesity meaningfully raise the risk of hospitalization for COVID-19 and mortality due to the disease [11]. Females generally have inherently resilient and changeable immune responses because of their higher number of X-chromosomes, which contain immune-related genes [1]; gender-reliant production of steroid

hormones [12]; and sex differences in angiotensin converting enzyme-2 (ACE-2) [13]. ACE-2 has lung protective effects by limiting angiotensin-2-mediated pulmonary capillary leakage and inflammation [14]. ACE-2 is also the primary target of the virus, and its expression level decreases with senility. In our female study population, advanced age was found to be associated with severe illness, and the threshold value was 47.

Another important imaging biomarker of a patient's physiologic reserve is body muscle mass and quality. Sarcopenia is a worsening of muscle mass and function and perhaps one of the most important issues associated with the pandemic. Globally, governments are applying actions, such as travel sanctions, isolation, separation, and public distancing, which are causing a prolonged sedentary life and hence sarcopenia. Additionally, alterations in nutritional consumption may enhance sarcopenia and increase body fat [15]. Another important factor is that COVID-19 infection itself causes acute sarcopenia [16]. Additionally, our study showed that sarcopenia detected during the initial evaluation is associated with severe disease. ROC analysis and regression analysis revealed that sarcopenia alone is as decisive as age. It can even provide more specific estimates.

Sarcopenia is affected by many factors, including age, physical activity, protein consumption, anabolic hormonal activity, and vitamin D levels [17,18]. Hormone decay (especially testosterone, oestrogen, and growth hormone) related to ageing contributes to muscle wasting [19]. Sarcopenia has been associated with reduced diaphragmatic muscle thickness [20]. Acute declines in diaphragmatic muscle thickness in hospitalized patients can provoke respiratory failure and necessitate prolonged mechanical ventilation in critically unwell patients [21]. In a recent study, to assess the relationship between clinical variables, pneumonia severity score, pectoralis muscle area, pectoralis muscle index, and patient outcomes (intubation, prolonged hospital stay, and death), chest computed tomography images of 130 COVID-19 patients were evaluated, and the pectoralis muscle index was found to be a predictor of prolonged hospital stay and death [4]. Our study also showed a negative impact of sarcopenia on the severity of pneumonia. For COVID-19, which has become a global epidemic, the fight against sarcopenia before and after the disease should be added to the fight against COVID-19. In the current study, HUAC was found to be as valuable as age.

CT imaging reveals fatty streaks within the muscles and permits analysis of muscle quality [22]. Lumbar, thoracic or cervical levels can be used [23]. Muscle cross-sectional area, muscle density and intramuscular adipose tissue area can be evaluated via CT, and lower densities are associated with high mortality [23,24]. Managing muscle health is important in COVID-19, as with any critical illness. Old

age, physical inactivity and insufficient protein consumption create an inclination to sarcopenia and insensitivity to anabolic stimuli [25]. Skeletal muscle produces myokines. Among them, interleukin (IL)-6 and IL-7 greatly affect the immune response [26]. It has been reported that preventive measures for frailty/sarcopenia can strengthen a patient's ability to fight COVID-19 [27]. The cytokine storm associated with COVID-19 may harm tissues directly and inhibit muscle protein synthesis [28]. Sarcopenia appears to play important roles in cause-and-effect relationships. In our study, we found that the HUAC value has the highest sensitivity in predicting moderate-severe pneumonia. At densities below 45 HU, the positive LR for having moderate-severe pneumonia was 2.08, the highest among the parameters studied. Bone density, another important metabolic biomarker, offered a high NPV value, although not the highest.

Bone is a tissue that has much contact with other tissues and possesses endocrine and paracrine functions important for metabolism, ageing and general health [29]. Opportunistic screening of metabolic bone disease on CT has been performed previously for the abdomen, pelvis, or lumbar spine, and bone density was assessed using Hounsfield units [10]. DXA, which is often used in daily routines, produces superpositional images and covers many anatomical structures. Therefore, a false elevated bone mineral density will be observed, and it will be challenging to predict the real risks to bone [10]. HU thresholds for L1 allow clinicians to screen for osteoporosis with >90% sensitivity and specificity using screening thresholds of 160 HU and 110 HU, respectively [30]. In our study, to predict moderate-severe pneumonia, the threshold was 183 HU, which provided a sensitivity of 68%, specificity of 49%, PPV of 46%, NPV of 70% and accuracy of 56%. Although bone density did not seem to contribute to the estimation of moderate-severe pneumonia in the regression analysis, statistically significant differences emerged in comparison of the various groups. In fact, the average bone density in the PCR-positive and non-pneumonia group was 221 HU, while the average density was 161 in the moderate-severe pneumonia group.

Another constitutional imaging biomarker may be breast hypertrophy in females, which has been related to high oestrogen levels [31]. Our study showed that the PCR-positive and non-pneumonia group had dense breast patterns at a rate of 67%, while the moderate-severe pneumonia group had a fatty breast pattern at a rate of 68%. This difference cannot be attributed to age alone. A correlation between oestradiol-estrone and mammographic density has been found for postmenopausal women [32]. Additionally, with ageing, a dense breast structure is not completely replaced by fat, and only some decreases in density are observed.

Obesity has been demonstrated to be an adverse prognostic factor in COVID-19 and is associated with an increased risk of hospitalization, critical care admission, and mortality [16]. The profuse fat content in obese patients overexpresses receptors for SARS-CoV-2, acts as a reservoir for viruses and supports the immune response [33]. Thus, patients with obesity may have a higher viral burden than lean patients, have more severe COVID-19, and usually take longer to convalesce [34]. In our study, SFT was directly correlated with the severity of the disease.

Our study was carried out at a time and in an environment in which a pandemic was underway and rapid virus transmission was occurring in the absence of vaccines. This study was conducted early in the pandemic and partly in an environment where CT was used in triage. Considering that CT is used in more selected cases today, it is therefore likely to represent a larger population. The current study is a screening perspective for clinical scenery and highlights the idea that warning images should be evaluated from a broad perspective. Additionally, patients have the right to know their silent conditions, such as osteoporosis, sarcopenia or osteosarcopenic obesity, as a requirement of personalized medicine.

Conclusions

In conclusion, the severity of COVID-19 pneumonia among adult females is associated with older age, lower bone density, lower HUAC value, greater SFT and fatty breast parenchyma. According to the regression analysis model created in this study, the effect of age and HUAC on development of moderate-to-severe COVID-19 pneumonia was 21%, and the contribution of constitutional factors was 21.9%. This is a substantial contribution to a disease that is affected by many factors and is currently a worldwide pandemic. Therefore, preventive medicine measures addressing conditions that affect the muscle quality of patients and the effects of age will gain more importance in the upcoming period.

Conflict of interest disclosure

There are no known conflicts of interest in the publication of this article. The manuscript was read and approved by all authors.

Compliance with ethical standards

Any aspect of the work covered in this manuscript has been conducted with the ethical approval of all relevant bodies and that such approvals are acknowledged within the manuscript.

Contributions

MS: Conceptualization; Data curation; Investigation; Formal analysis; Methodology; Project administration; Resources; Supervision; Validation; Visualization; Writing – original draft; Writing – review & editing.

MD: Data curation; Formal analysis; Investigation; Methodology; Writing – review & editing.

CE, IDS: Data curation; Formal analysis; Investigation; Methodology; Project administration; Resources; Supervision; Validation; Visualization; Writing – original draft; Writing – review & editing.

References

1. Qian J, Zhao L, Ye RZ, Li XJ, Liu YL. Age-dependent Gender Differences in COVID-19 in Mainland China: Comparative Study. *Clin Infect Dis*. 2020;71(9):2488-2494. doi:10.1093/cid/ciaa683
2. Öztürk R, Taşova Y, Ayaz A. COVID-19: pathogenesis, genetic polymorphism, clinical features and laboratory findings. *Turk J Med Sci*. 2020;50(SI-1):638-657. Published 2020 Apr 21. doi:10.3906/sag-2005-287
3. Antonello RM, Dal Bo E, De Cristofaro P, Luzzati R, Di Bella S. The seXY side of COVID-19: what is behind female protection?. *Infez Med*. 2020;28(2):288-289.
4. Ufuk F, Demirci M, Sagtas E, Akbudak IH, Ugurlu E, Sari T. The prognostic value of pneumonia severity score and pectoralis muscle Area on chest CT in adult COVID-19 patients. *Eur J Radiol*. 2020;131:109271. doi:10.1016/j.ejrad.2020.109271
5. Pradhan A, Olsson PE. Sex differences in severity and mortality from COVID-19: are males more vulnerable?. *Biol Sex Differ*. 2020;11(1):53. Published 2020 Sep 18. doi:10.1186/s13293-020-00330-7
6. Xu K, Chen Y, Yuan J, et al. Factors Associated With Prolonged Viral RNA Shedding in Patients with Coronavirus Disease 2019 (COVID-19). *Clin Infect Dis*. 2020;71(15):799-806. doi:10.1093/cid/ciaa351
7. Zheng S, Fan J, Yu F, et al. Viral load dynamics and disease severity in patients infected with SARS-CoV-2 in Zhejiang province, China, January-March 2020: retrospective cohort study. *BMJ*. 2020;369:m1443. Published 2020 Apr 21. doi:10.1136/bmj.m1443
8. Ai T, Yang Z, Hou H, et al. Correlation of Chest CT and RT-PCR Testing for Coronavirus Disease 2019 (COVID-19) in China: A Report of 1014 Cases. *Radiology*. 2020;296(2):E32-E40. doi:10.1148/radiol.2020200642
9. Tabatabaei SMH, Rajebi H, Moghaddas F, Ghasemiadl M, Talari H. Chest CT in COVID-19 pneumonia: what are the findings in mid-term follow-up?. *Emerg Radiol*. 2020;27(6):711-719. doi:10.1007/s10140-020-01869-z
10. Hendrickson NR, Pickhardt PJ, Del Rio AM, Rosas HG, Anderson PA. Bone Mineral Density T-Scores Derived from CT Attenuation Numbers (Hounsfield Units): Clinical Utility and Correlation with Dual-energy X-ray Absorptiometry. *Iowa Orthop J*. 2018;38:25-31.

11. Muniyappa R, Gubbi S. COVID-19 pandemic, coronaviruses, and diabetes mellitus. *Am J Physiol Endocrinol Metab.* 2020;318(5):E736-E741. doi:10.1152/ajpendo.00124.2020
12. Klein SL, Flanagan KL. Sex differences in immune responses. *Nat Rev Immunol.* 2016;16(10):626-638. doi:10.1038/nri.2016.90
13. The Lancet. The gendered dimensions of COVID-19. *Lancet.* 2020;395(10231):1168. doi:10.1016/S0140-6736(20)30823-0
14. Dhochak N, Singhal T, Kabra SK, Lodha R. Pathophysiology of COVID-19: Why Children Fare Better than Adults?. *Indian J Pediatr.* 2020;87(7):537-546. doi:10.1007/s12098-020-03322-y
15. Kirwan R, McCullough D, Butler T, Perez de Heredia F, Davies IG, Stewart C. Sarcopenia during COVID-19 lockdown restrictions: long-term health effects of short-term muscle loss. *Geroscience.* 2020;42(6):1547-1578. doi:10.1007/s11357-020-00272-3
16. Welch C, Greig C, Masud T, Wilson D, Jackson TA. COVID-19 and Acute Sarcopenia. *Aging Dis.* 2020;11(6):1345-1351. Published 2020 Dec 1. doi:10.14336/AD.2020.1014
17. Brioché T, Pagano AF, Py G, Chopard A. Muscle wasting and aging: Experimental models, fatty infiltrations, and prevention. *Mol Aspects Med.* 2016;50:56-87. doi:10.1016/j.mam.2016.04.006
18. Vezzoli A, Mrakic-Spota S, Montorsi M, et al. Moderate Intensity Resistive Training Reduces Oxidative Stress and Improves Muscle Mass and Function in Older Individuals. *Antioxidants (Basel).* 2019;8(10):431. doi:10.3390/antiox8100431
19. Marty E, Liu Y, Samuel A, Or O, Lane J. A review of sarcopenia: Enhancing awareness of an increasingly prevalent disease. *Bone.* 2017;105:276-286. doi:10.1016/j.bone.2017.09.008
20. Deniz O, Cotelis S, Karatoprak NB, et al. Diaphragmatic muscle thickness in older people with and without sarcopenia. *Aging Clin Exp Res.* 2021;33(3):573-580. doi:10.1007/s40520-020-01565-5
21. Supinski GS, Morris PE, Dhar S, Callahan LA. Diaphragm Dysfunction in Critical Illness. *Chest.* 2018; 153(4):1040-1051. doi:10.1016/j.chest.2017.08.1157
22. Engelke K, Museyko O, Wang L, Laredo JD. Quantitative analysis of skeletal muscle by computed tomography imaging-State of the art. *J Orthop Translat.* 2018;15:91-103. doi:10.1016/j.jot.2018.10.004
23. Giraudo C, Cavaliere A, Lupi A, Guglielmi G, Quaia E. Established paths and new avenues: a review of the main radiological techniques for investigating sarcopenia. *Quant Imaging Med Surg.* 2020;10(8):1602-1613. doi:10.21037/qims.2019.12.15
24. Erlandson MC, Lorbergs AL, Mathur S, Cheung AM. Muscle analysis using pQCT, DXA and MRI. *Eur J Radiol.* 2016;85(8):1505-1511. doi:10.1016/j.ejrad.2016.03.001
25. Nilsson MI, Mikhail A, Lan L, et al. A Five-Ingredient Nutritional Supplement and Home-Based Resistance Exercise Improve Lean Mass and Strength in Free-Living Elderly. *Nutrients.* 2020;12(8):2391. Published 2020 Aug 10. doi:10.3390/nu12082391
26. Pedersen BK, Febbraio MA. Muscles, exercise and obesity: skeletal muscle as a secretory organ. *Nat Rev Endocrinol.* 2012;8(8):457-465. Published 2012 Apr 3. doi:10.1038/nrendo.2012.49
27. Ekiz T, Kara M, Özcan F, Ricci V, Özçakar L. Sarcopenia and COVID-19: A Manifold Insight on Hypertension and the Renin Angiotensin System. *Am J Phys Med Rehabil.* 2020;99(10):880-882. doi:10.1097/PHM.0000000000001528
28. Zhou L, Liu C, Yang C. Comment on 'COVID-19: a major cause of cachexia and sarcopenia' by Morley et al. *J Cachexia Sarcopenia Muscle.* 2021;12(1):233-234. doi:10.1002/jcsm.12648
29. Aparisi Gómez MP, Ayuso Benavent C, Simoni P, Aparisi F, Guglielmi G, Bazzocchi A. Fat and bone: the multiperspective analysis of a close relationship. *Quant Imaging Med Surg.* 2020;10(8):1614-1635. doi:10.21037/qims.2020.01.11
30. Pickhardt PJ, Pooler BD, Lauder T, del Rio AM, Bruce RJ, Binkley N. Opportunistic screening for osteoporosis using abdominal computed tomography scans obtained for other indications. *Ann Intern Med.* 2013;158(8):588-595. doi:10.7326/0003-4819-158-8-201304160-00003
31. Kilbreath S, Refshauge KM, Beith J, et al. Prevention of osteoporosis as a consequence of aromatase inhibitor therapy in postmenopausal women with early breast cancer: rationale and design of a randomized controlled trial. *Contemp Clin Trials.* 2011;32(5):704-709. doi:10.1016/j.cct.2011.04.012
32. Greendale GA, Palla SL, Ursin G, et al. The association of endogenous sex steroids and sex steroid binding proteins with mammographic density: results from the Postmenopausal Estrogen/Progestin Interventions Mammographic Density Study. *Am J Epidemiol.* 2005;162(9):826-834. doi:10.1093/aje/kwi286
33. Ritter A, Kreis NN, Louwen F, Yuan J. Obesity and COVID-19: Molecular Mechanisms Linking Both Pandemics. *Int J Mol Sci.* 2020;21(16):5793. Published 2020 Aug 12. doi:10.3390/ijms21165793
34. Zabulienė L, Ilias I. Obesity, abdominal organ size and COVID-19 severity. *Med Hypotheses.* 2020;144:110279. doi:10.1016/j.mehy.2020.110279